Electronic Supplementary Material (ESI) for Inorganic Chemistry Frontiers.

Self-Promoted Ammonia Selectivity for the Electro-Reduction of Nitrogen on *gt*-C_3N_4 Supported Single Metal Catalysts: The Machine Learning Model and Physical Insights

Lifu Zhang[a,b,†], *Lanlan Chen*[b,†], *Wanghui Zhao*[b,†], *Zhenpeng Hu**[a,], *Jing Chen*[a,c], *Wenhua Zhang**[b], *and Jinlong Yang*[b]

[a] *School of Physics, Nankai University, Tianjin 300071, China*

[b] *Hefei National Laboratory for Physical Sciences at the Microscale, CAS Key Laboratory of Materials for Energy Conversion and Synergetic Innovation Centre of Quantum Information & Quantum Physics, University of Science and Technology of China, Hefei, Anhui 230026, China*

[c] *Collaborative Innovation Center of Extreme Optics, Shanxi University, Taiyuan, Shanxi 030006, China*

Table S1. The reaction energy (ΔE/eV) of the adsorption of H, N_2 and the protonation of nitrogen on Mo/Re embedded MoS_2.

System	*ΔE/eV*									
	*H	*NN	*NNH	*NN*H	*1N_2-NN	*1N_2-NNH	*1N_2-NN*H	*2N_2-NN	*2N_2-NNH	*2N_2-NN*H
Mo/ MoS_2	-0.36	-1.09	0.25	-0.30	-1.20	0.33	-0.18	-1.25	1.02	1.09
Re/ MoS_2	-0.68	-1.55	0.15	-0.60	-1.33	0.40	-0.68	-0.67	1.25	1.65

Table S2. The reaction free energy (ΔG/eV) of the adsorption of H, N_2 and the protonation of nitrogen on different element embedded *gt*-C_3N_4.

Element	*ΔG/eV*											
	*H	*NN	*NN	*NNH	*NNH	*NN*H	*1N_2-NN	*1N_2-NNH	*1N_2-NN*H	*2N_2-NN	*2N_2-NNH	*2N_2-NN*H
Sc	-0.80	-0.48	-0.53				-0.19			-0.04		
Ti	-0.63	-0.73	-0.75	0.93	0.53	0.01	-0.51	1.15	0.63	-0.29	1.04	0.93
V	-0.69	-0.88	-0.78	0.93	0.62	0.06	-0.50	1.13	0.35	-0.35	0.83	1.05
Cr	-0.32	-0.92	-0.40	1.04	0.63	0.19	-0.12	0.98	0.14	-0.70	1.26	1.79
Mn	-0.53	-0.52	-0.24	1.05	0.95	0.32	-0.17	1.13	0.08	-0.32	1.75	2.52
Fe	-0.39	-0.89	-0.54	1.18	1.12	0.23	0.01			0.54		
Co	-0.35	-0.77	-0.35	1.25	1.24	0.20	0.37			0.48		
Ni	0.00	-0.82	-0.29	1.55	1.50	0.65	0.04			0.76		
Cu	-0.27	-0.52	0.00	1.92	1.87	0.75	*					
Zn	-0.35	0.41	0.45									
Y	-0.61	-0.20	-0.32				-0.21			-0.04		
Zr	-0.82	-0.77	-0.87	0.69	0.32	-0.37	-0.60	0.98	0.21	-0.37	0.88	0.44
Nb	-0.67	-0.85	-0.85	0.68	0.28	-0.12	-0.72	0.74	0.34	-0.53	0.57	0.41
Mo	-0.61	-1.18	-1.08	0.82	0.85	-0.04	-1.01	1.08	0.48	-0.71	1.04	1.15
Tc	-0.71	-1.23	-0.69	0.97	0.67	-0.39	-1.01	1.24	0.02	-0.58	1.84	2.23
Ru	-0.79	-1.01	-0.39	0.97	0.63	-0.65	-0.84	1.21	-0.43	0.43		
Rh	-0.52	-1.00	-0.35	0.90	0.51	-0.52	-0.49					
Pd	-0.32	-1.00	-0.66	1.90	1.76	0.80	0.36					
Ag	-0.23	0.35	0.35‡									
Cd	0.62	0.40	0.45									
Ta	-1.17	-1.08	-1.30	0.56	0.07	-0.59	-0.94	0.63	0.00	-0.76	0.49	0.29
W	-1.19	-1.29	-1.56	0.45	0.61	-0.64	-1.32	0.81	0.07	-1.01	0.87	0.92
Re	-1.26	-1.42	-1.15	0.58	0.43	-0.84	-1.33	0.91	-0.44	-0.98	1.58	2.14

*NN*H represents the geometry where one nitrogen is adsorbed on the metal, when H is also adsorbed on the metal. * represent the structure does not exist.

Table S3. PDS and U_L for *gt*-C_3N_4 supported different element-N_2 complex to catalyse N_2-fixation.

Element	**2N_2-NN*	
	PDS	U_L
V	*2N_2-NN + (H^++e^-) → *2N_2-NNH	-0.83
Cr	*2N_2-NN + (H^++e^-) → *2N_2-NNH	-1.26
Mo	*2N_2-NN + (H^++e^-) → *2N_2-NNH	-1.04
W	*2N_2-NN + (H^++e^-) → *2N_2-NNH	-0.87

Table S4. Net effective charges calculated from Bader Charge analysis of the systems on the H@Sc/*gt*-C_3N_4, 1N_2-H@Rh/*gt*-C_3N_4, 2N_2-H@Ru/*gt*-C_3N_4, 3N_2-H@Zr/*gt*-C_3N_4 which correspond to low selectivity, and H@V/*gt*-C_3N_4, 1N_2-H@V/*gt*-C_3N_4, 2N_2-H@V/*gt*-C_3N_4 and 3N_2-H@V/*gt*-C_3N_4 which correspond to high selectivity.

	Bader valence				Bader valence			
	H@Sc/*gt*-C_3N_4	$1N_2$-H@Rh/*gt*-C_3N_4	$2N_2$-H@Ru/*gt*-C_3N_4	$3N_2$-H@Zr/*gt*-C_3N_4	H@V/*gt*-C_3N_4	$1N_2$-H@V/*gt*-C_3N_4	$2N_2$-H@V/*gt*-C_3N_4	$3N_2$-H@V/*gt*-C_3N_4
metal	Sc：+1.87	Rh：+0.50	Ru：+1.04	Zr：+2.01	V：+1.36	V：+1.42	V：+1.42	V：+1.45
H on metal	-0.65	-0.16	-0.18	-0.41	-0.52	-0.47	-0.41	-0.20
adsorbed N_2		-0.34/+0.12	-0.29/+0.09 -0.24/+0.04	-0.38/+0.14 -0.38/+0.07 -0.36/+0.11		-0.26/-0.01	-0.25/+0.01 -0.39/+0.15	-0.26/+0.03 -0.31/+0.05 -0.26/+0.03

Table S5. Net effective charges calculated from Bader Charge analysis of TM/*gt*-C_3N_4.

	Bader valence of metal									
	Sc/*gt*-C_3N_4	Ti/*gt*-C_3N_4	V/*gt*-C_3N_4	Cr/*gt*-C_3N_4	Mn/*gt*-C_3N_4	Fe/*gt*-C_3N_4	Co/*gt*-C_3N_4	Ni/*gt*-C_3N_4	Cu/*gt*-C_3N_4	Zn/*gt*-C_3N_4
substrate	+1.45	+1.18	+1.03	+0.95	+0.79	+0.90	+0.75	+0.63	+0.65	+0.11
*NN		+1.42	+1.38	+1.15	+1.15	+1.03	+0.86	+0.67	+0.83	
*$1N_2$-NN		+1.48	+1.41	+1.26	+1.11					
*$2N_2$-NN		+1.51	+1.45	+1.28	+1.21					
	Bader valence of metal									
	Y/*gt*-C_3N_4	Zr/*gt*-C_3N_4	Nb/*gt*-C_3N_4	Mo/*gt*-C_3N_4	Tc/*gt*-C_3N_4	Ru/*gt*-C_3N_4	Rh/*gt*-C_3N_4	Pd/*gt*-C_3N_4	Ag/*gt*-C_3N_4	Cd/*gt*-C_3N_4
substrate	+1.44	+1.65	+1.35	+1.02	+0.84	+0.67	+0.52	+0.17	+0.20	+0.11
*NN		+1.77	+1.63	+1.22	+1.07	+0.81	+0.47	+0.29		
*$1N_2$-NN		+1.85	+1.72	+1.35	+1.19	+0.97				
*$2N_2$-NN		+1.92	+1.87	+1.41	+1.28					
	Bader valence of metal									
			Ta/*gt*-C_3N_4	W/*gt*-C_3N_4	Re/*gt*-C_3N_4					
substrate			+1.32	+0.97	+0.80					
*NN			+1.61	+1.41	+1.15					
*$1N_2$-NN			+1.78	+1.56	+1.38					
*$2N_2$-NN			+1.84	+1.64	+1.50					

Table S6. Net effective charges calculated from Bader Charge analysis of the systems on the $1N_2$@V/*gt*-C_3N_4, $2N_2$@V/*gt*-C_3N_4 and $3N_2$@V/*gt*-C_3N_4.

	Bader valence		
	$1N_2$@V/*gt*-C_3N_4	$2N_2$@V/*gt*-C_3N_4	$3N_2$@V/*gt*-C_3N_4
adsorbed N_2	-0.40/+0.01	-0.40/+0.08 - 0.37/+0.05	-0.29/+0.02 - 0.30/+0.02 -0.38/+0.10

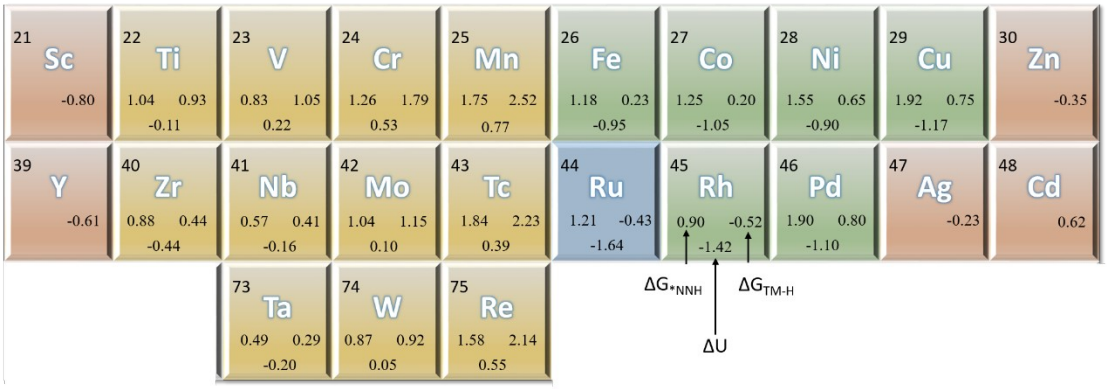

Figure S1. Numbers of nitrogen molecules effectively binding on TM/*gt*-C_3N_4(orange, green, blue and yellow region represent 0, 1, 2, 3), the reaction Gibbs free energy (eV) of the formation of *NNH(ΔG_{*NNH}), the adsorption free energy of H on the metal for TM/*gt*-C_3N_4 (ΔG_{TM-H}), and the potential difference (U) between the formation of *NNH and TM-H ($\Delta U = U_{*NNH} - U_{TM-H} = -\Delta G_{*NNH}/e - [-\Delta G_{TM-H}/e]$).

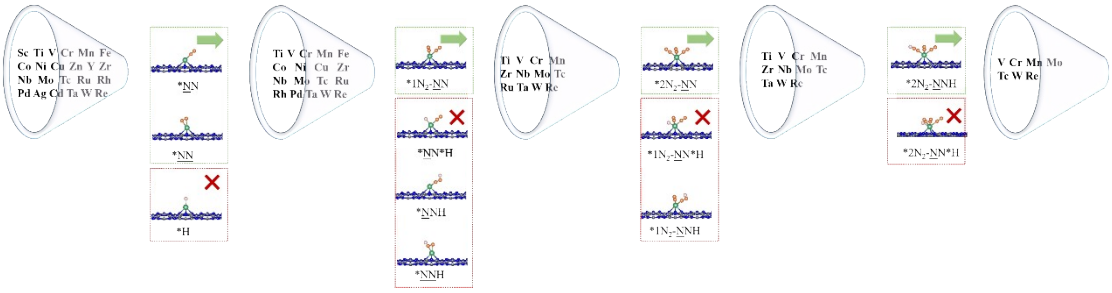

Figure S2. Flowchart of the screening procedure of eNRR on TM/*gt*-C_3N_4.

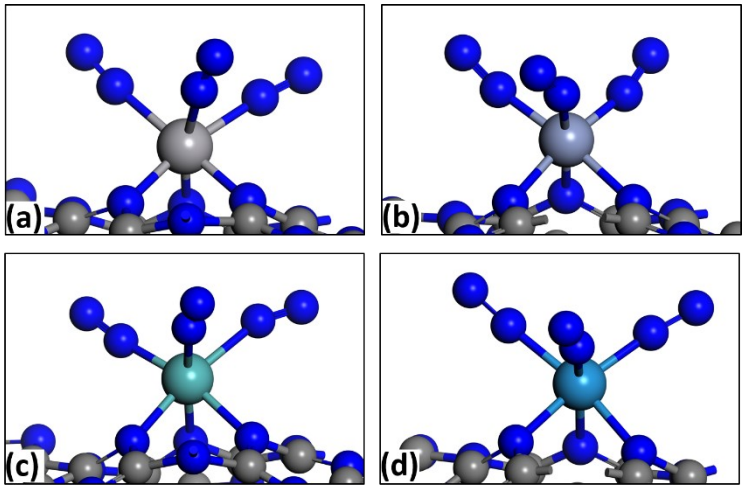

Figure S3. Structural snapshots of the (a) $3N_2$@V/*gt*-C_3N_4, (b) $3N_2$@Cr/*gt*-C_3N_4, (c) $3N_2$@Mo/*gt*-C_3N_4, and (d) $3N_2$@W/*gt*-C_3N_4 for AIMD simulation at 300 K after 5.0 ps.

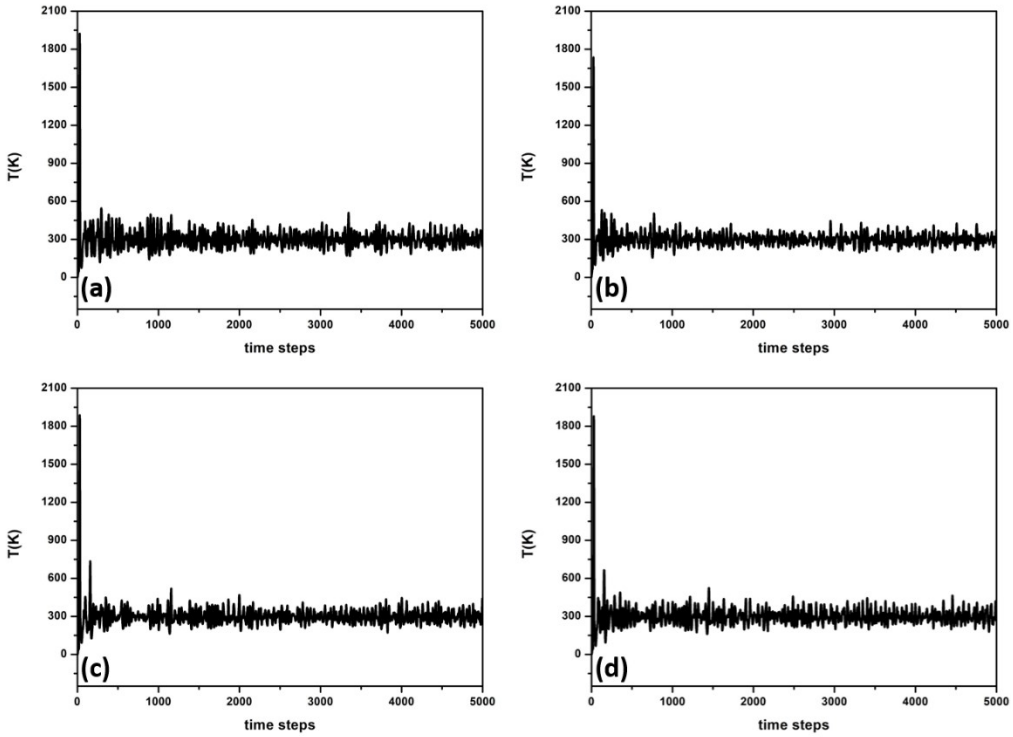

Figure S4. Temperature vs time for (a) $3N_2$@V/*gt*-C_3N_4, (b) $3N_2$@Cr/*gt*-C_3N_4, (c) $3N_2$@Mo/*gt*-C_3N_4, and (d) $3N_2$@W/*gt*-C_3N_4 during the MD simulation after 5.0 ps.

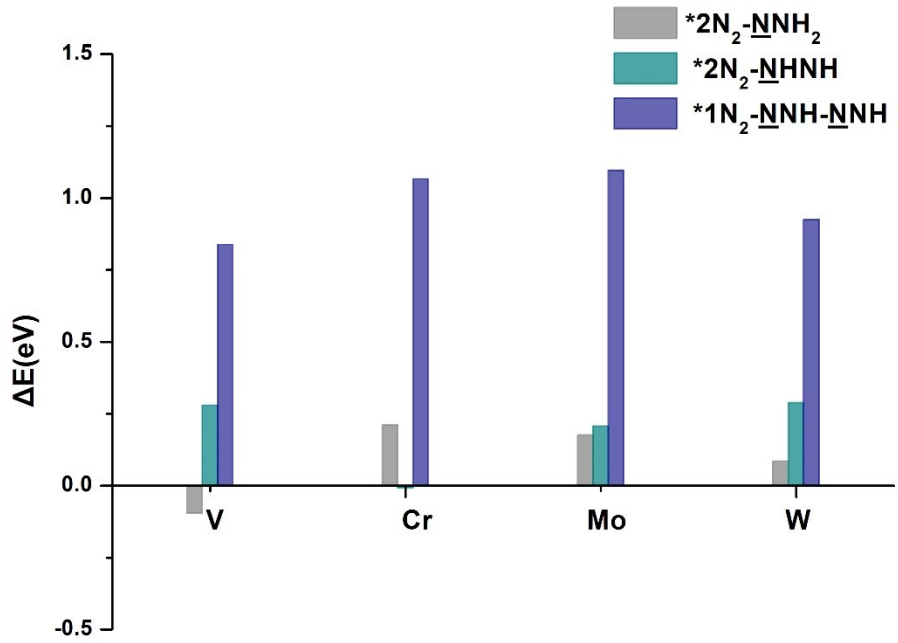

Figure S5. The energy of the second protonation of nitrogen for $3N_2$ adsorbed on TM/*gt*-C_3N_4 (TM = V, Cr, Nb, Mo, Ta, and W).

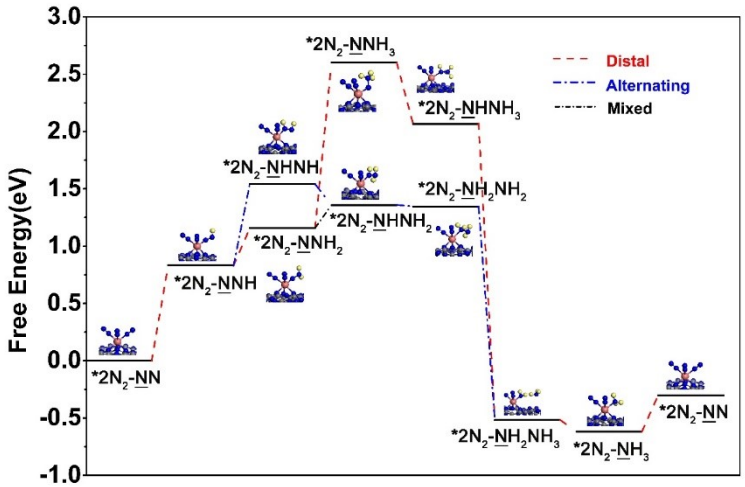

Figure S6. Free energy diagram at U = 0 V (vs SHE) for the reaction intermediates by adsorbing three N_2 on the V/*gt*-C_3N_4. The dashed lines indicated the possible reaction pathways.

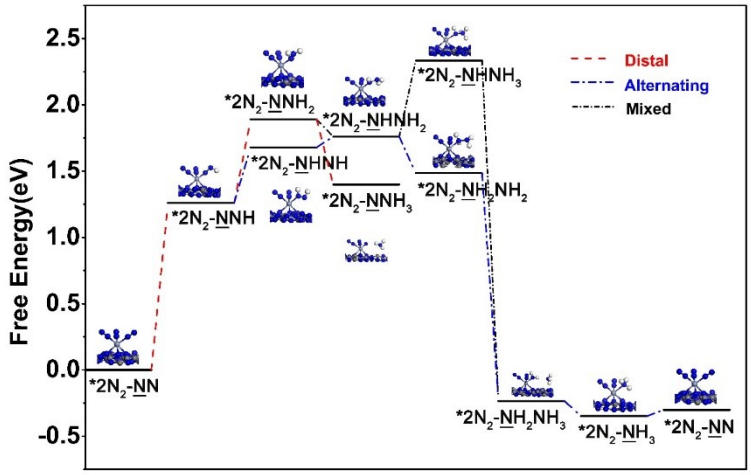

Figure S7. Free energy diagram at U = 0 V (vs SHE) for the reaction intermediates by adsorbing three N_2 on the Cr/*gt*-C_3N_4. The dashed lines indicated the possible reaction pathways.

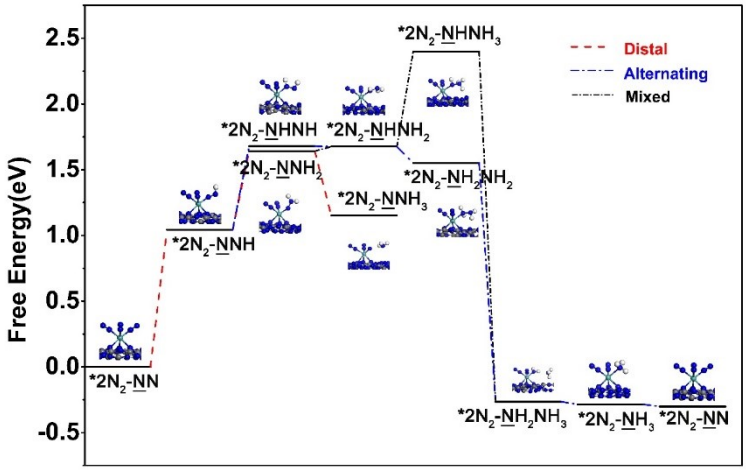

Figure S8. Free energy diagram at U = 0 V (vs SHE) for the reaction intermediates by adsorbing three N_2 on the Mo/*gt*-C_3N_4. The dashed lines indicated the possible reaction pathways.

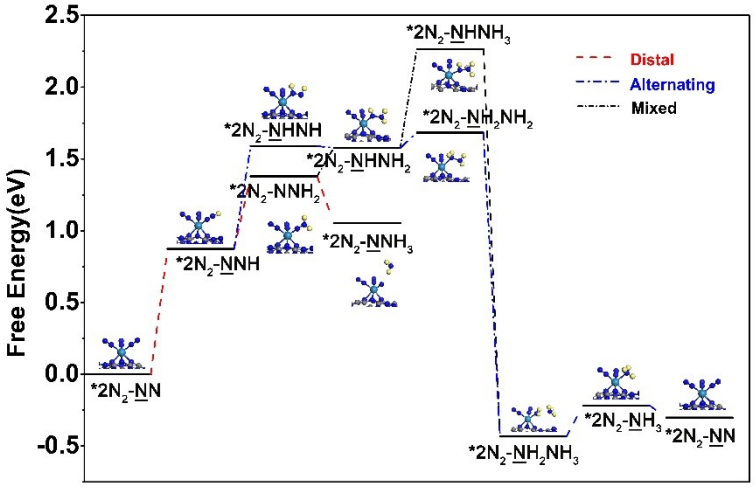

Figure S9. Free energy diagram at U = 0 V (vs SHE) for the reaction intermediates by adsorbing three N_2 on the W/*gt*-C_3N_4. The dashed lines indicated the possible reaction pathways.

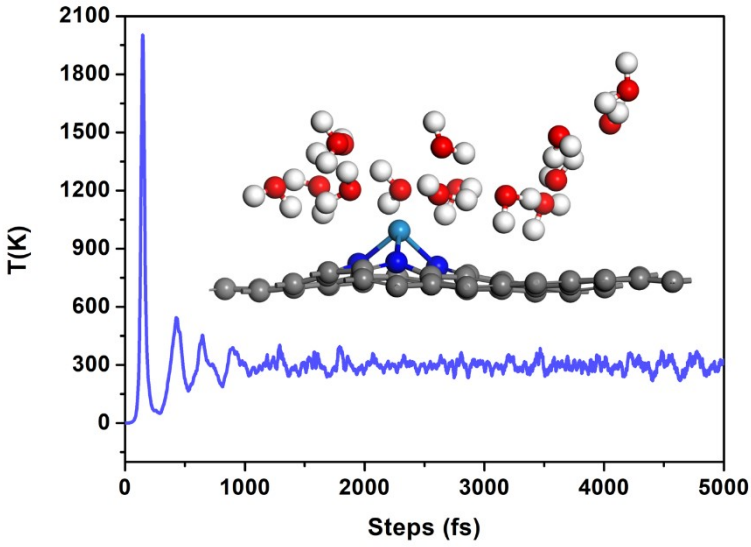

Figure S10. Molecular dynamics simulation at T = 300 K with 5 ps.